Indonesian Journal of Electrical Engineering and Informatics (IJEEI)
Vol. 12, No. 3, September 2024, pp. 543~557
ISSN: 2089-3272, DOI: 10.52549/ijeei.v12i3.5472

Regulation of Active and Reactive Powers in Doubly-Fed Induction Generators Utilizing Proportional-Integral and Artificial Neural Network Controllers

Mohammed Bouzidi[1], Abdelfatah Nasri[2], Oussama Hafsi[3], Boubakar Faradji[4]
[1,4]Energy and Materials Laboratory, University of Tamanghasset, Algeria
[2]laboratory Smart Grid and Renewable Energy SGRE University Tahri Mohamed Bechar Algeria
[3]Department of Electrical Engineering, LDDI Laboratory, Ahmed Draia University, Adrar, Algeria

Article Info

Article history:

Received Mar 1, 2024
Revised Sep 1, 2024
Accepted Sep 8, 2024

Keywords:

DFIG Control
Neural Control
Active and Reactive Power
Wind Turbines
PI Control

ABSTRAC T

In this paper, vector orientation and neural networks are used to simulate and regulate a Doubly Fed Induction Generator (DFIG) wind turbine. The aerodynamic turbine and DFIG dq models are developed. PI current regulation is used in vector control to separate active and reactive power control. To reproduce the PI response, training networks create a different neural vector control scheme. Comparative simulations confirm the effectiveness of both control methods in following set points and counteracting disturbances. The neural vector control scheme outperforms the PI scheme in managing short-term changes. In contrast to the PI control, it has quicker response times for both rising and settling. Neural vector control enables precise and rapid tracking of electromagnetic torque. Neural vector control could improve the performance of DFIG wind turbines because it has an adaptive architecture that lets it respond well to changes in parameters and maintain its accuracy over time. Additional investigation is needed to improve neural network training techniques and incorporate them with conventional control systems.

Corresponding Author:

Mohammed Bouzidi,
Department of Sciences and Technology,
Faulty of Sciences and Technology,
University of Tamanghasset, Algeria
Email: mohbouzidi81@yahoo.fr

NOMENCLATURE / SYMBOLS

DFIG	Doubly .fed induction generator	(Idr ,Iqr),(Ids ,Iqs)	Components (d,q) of rotor and Stator current
PWM	Pulse Width .Modulation	(Vdr ,Vqr),(Vds ,Vqs)	Components (d,q) of rotor and Stator voltage
ANN	Artificial Neuron Network	Rs ,Rr	Statoric and rotoric winding resistors
CLTF	Closed Loop Transfer Function	[Msr]	Matrix of stator-rotor mutual inductors
Lm	Magnetizing inductance	Cem	Electromagnetic torque
[Lss]	Stator Inductor Matrix	(φdr , φqr)	d and q components of rotor flux.
[Lrr]	Rotor Inductor Matrix	Ls	Stator Cyclic Clean Inductance
Q	Reactive Power	Lr	Rotor Cyclic Clean Inductance
P	Active power	(φds , φqs)	d and q components of stator flux.

1. INTRODUCTION

Double-fed induction machines (DFIG) are frequently used in variable-speed wind turbines. DFIG optimizes power capture from fluctuating winds by adjusting rotor speed. Both the stator and rotor regulate rotor excitation, allowing for variable-speed operation. DFIG provides advantages in converter size compared to direct-drive synchronous generators. Sophisticated control enhances the performance of Doubly Fed Induction Generators under changing wind conditions. The dual-fed induction machine has been thoroughly studied in electro-technical labs to understand its evolution and application areas [1], [2]. Contemporary drive systems necessitat4e accurate and uninterrupted regulation of speed, torque, and position while also

guaranteeing stability, responsiveness, and optimal efficiency. Since the 1960s, advancements in power electronic components and computing have gradually replaced traditional generation systems with more advanced static converters, allowing for better control of electrical machines [3], [4].Utilizing a dual-fed induction machine (DFIG), which powers the stator with a constant supply and the rotor with a variable supply, is a new strategy for high-power applications [5], [6].

To match the performance of the DC machine, it is necessary to separate the flux and electromagnetic torque. As a result, field-oriented control technology was developed. The objective is to implement vector control on a transformer-powered rotor and control the Doubly Fed Induction Machine (DFIM), which functions like a DC machine with separate flux and torque. A variety of linear and nonlinear control technologies, both conventional and AI-based, have been created for industrial use, providing easy operation, setup, and management [7], [8].A lot of people have studied doubly-fed induction generators, such as H. Benbouhenni et al. [9], Abdulghafour H. et al.[10], Modeling and Control of a Wind Turbine Based on a DFIG [11], F. Moulay et al.[12], M. Lamnadi et al. [13], and Nathan O.F. [14]. They have examined their behavior in relation to rotor and stator currents and methods for regulating their speed. Various control strategies have been examined, such as vector control, direct torque control, model predictive control, and artificial intelligence techniques.

The objective is to attain optimal variable-speed operation, enhance power capture from varying wind speeds, maintain stability during grid disturbances, and enhance overall performance and efficiency. Simulation and experimental results have been shown for various DFIG control strategies. The results offer valuable information for creating sophisticated control systems to maximize the efficiency of DFIG-based wind turbines. Opportunities for innovation in this field persist through new methods such as machine learning and model-free control paradigms [15], [16], [17].

This paper seeks to analyze and regulate a DFIG incorporated into a wind turbine through the application of artificial intelligence methods. The article provides an in-depth examination of the DFIG-based wind energy conversion system, which involves modeling the wind turbine powering the DFIG. The system comprises a DFIG that is directly connected to the power system. Vector control is used to independently adjust active and reactive power by aligning the stator flux. Neural network control is implemented to enhance the robustness of DFIG controllers against parameter variations. By comparing their performance, it was found that direct neural network control with neural PI regulators was better than conventional vector control with PI regulators. Industry benchmark references from the literature were used to validate the simulation results.

2. MODELING AND DESCRIBING THE SYSTEM

Figure 1 illustrates the entire system, which consists of two converters: a rectifier and an inverter. as referenced in source . An in-depth evaluation and analysis of the mathematical model of the electrical system are crucial for effective management. This entails examining particular assumptions to create a streamlined model [18].

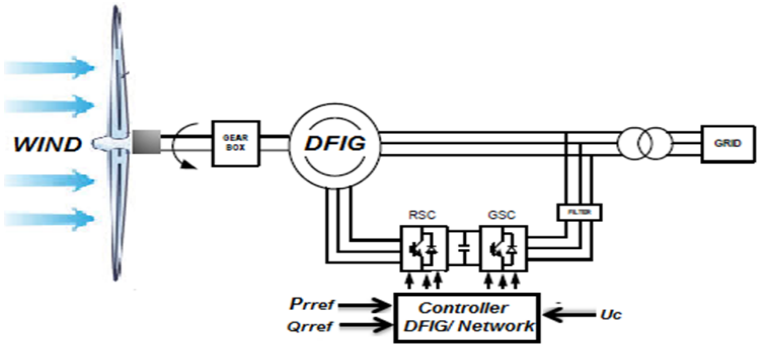

Figure 1. Wind energy system using DFIG

2.1. Wind Turbine modeling

Turbines can be oriented with either vertical or horizontal axes. Contemporary turbines typi-cally feature a horizontal axis with two or three blades and can be oriented towards or away from the wind. The kinetic energy of air particles moving through the turbines swept area, S, is what produces wind power. The mechanical power can be represented as [12], [19]:

$$P_{aer} = C_p . P_v = \frac{1}{2}\rho . \pi R^2 . V^3 . C_p(\lambda, \beta) \quad (1)$$

Where the power coefficient, Cp(λ,β), is dependent on the pitch angle β and the tip speed ratio λ. The air density is represented by ρ, the rotor radius by R, the wind speed by V.

The blade speed to wind speed ratio is known as the tip speed ratio [12], [19]:

$$\lambda = \frac{\omega_{turbine}}{V} * R \quad (2)$$

Where: $\omega_{turbine}$ is the angular speed of the wind turbine rotor.

Albert Betz determined the maximum power coefficient Cp in 1920 to be:

$$C_{pmax} = \frac{P_{max}}{P_{aer}} \approx 0.59 \quad (3)$$

An analytical formula for determining the (Cp=f(λ,b)) of high-speed rotating wind turbines with 2 or 3 blades is provided by equation (4). This formula relies on empirical data from sources [13] and [20].

$$C_p = f(\lambda, \beta) = (0.3 - 0.00167 . \beta) . \sin\left(\frac{\pi.(\lambda+0.1)}{10-0.3\beta}\right) - 0.00184(\lambda - 3) \quad (4)$$

Figure (2) displays the relationship C_p and λ for different blade pitch angles.

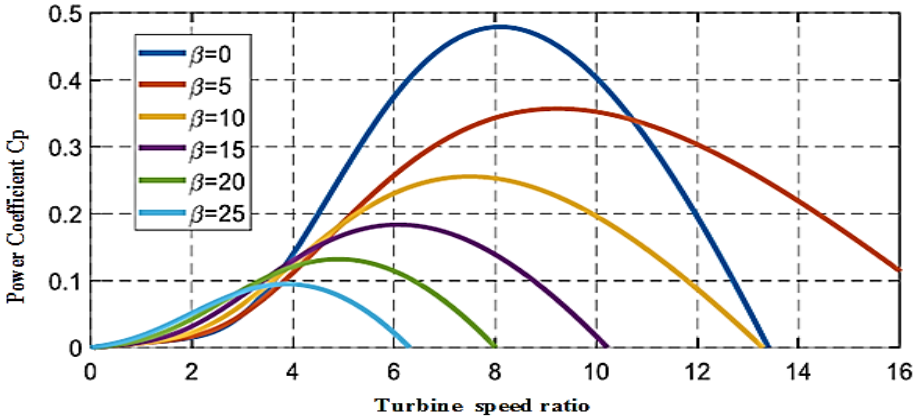

Figure 2. Function of tip speed ratio (λ) on aerodynamic coefficient

The aerodynamic torque is directly determined by the turbine speed, according to reference [13] .

$$C_{aer} = \frac{P_{aer}}{\omega_{turbine}} = C_p * P_v = \frac{1}{2}\rho\pi R^2 V^3 C_p(\lambda, \beta) . \frac{1}{\omega_{turbine}} \quad (5)$$

Total inertia J includes referred turbine inertia and generator inertia [21], [22].

$$J = \frac{J_{turbine}}{G^2} + J_g \quad (6)$$

Where: $J_{turbine}$ and Jg represent the inertia of the turbine and the generator, respectively.

The fundamental dynamic equation evaluates the variation in mechanical speed by assessing the total mechanical torque (Cmec) acting on the rotor. This total torque is made up of the electromagnetic torque (Cem) from the generator, along with the viscous friction and gearbox torques. [12]

$$C_{mec} = C_{aer} - C_{em} - C_{vis} \quad (7)$$

$$C_{mec} = C_{aer} - C_{em} - f . \omega_{mec} \quad (8)$$

The variables C_{mec} , C_{aer} ,f, and ω_{mec} are represent electromagnetic torque, aerodynamic torque, friction, and mechanical speed of DFIG, respectively.

2.2. Modeling DFIG

Two-phase d-q models acquired through Park transformation are frequently utilized to enhance the modeling of doubly fed induction generators. The dynamic model in the d-q frame comprises electrical equations (9) and magnetic equations (10). [8], [11], [23].

$$\begin{cases} V_{sd} = R_s I_{sd} + \frac{d\varphi_{sd}}{dt} - \varphi_{sq}.\omega_s \\ V_{sq} = R_s I_{sd} + \frac{d\varphi_{sq}}{dt} - \varphi_{sd}.\omega_s \\ V_{rd} = R_r I_{rd} + \frac{d\varphi_{rd}}{dt} - \varphi_{rq}.(\omega_s - \omega_r) \\ V_{rq} = R_r I_{rd} + \frac{d\varphi_{rq}}{dt} - \varphi_{rd}.(\omega_s - \omega_r) \\ \omega_s = \frac{d\theta_s}{dt} \end{cases} \quad (9)$$

$$\begin{cases} \varphi_{ds} = L_s I_{ds} + M_{sr} I_{dr} \\ \varphi_{qs} = L_s I_{qs} + M_{sr} I_{qr} \\ \varphi_{dr} = L_r I_{dr} + M_{sr} I_{ds} \\ \varphi_{qr} = L_r I_{qr} + M_{sr} I_{qs} \\ \omega_s = \frac{d\theta_s}{dt} \end{cases} \quad (10)$$

The expressions for the currents in terms of the fluxes are as follows:

$$\begin{cases} I_{ds} = \frac{1}{\sigma L_s}\varphi_{ds} - \frac{M_{sr}}{\sigma L_s L_r}\varphi_{dr} \\ I_{qs} = \frac{1}{\sigma L_s}\varphi_{qs} - \frac{M_{sr}}{\sigma L_s L_r}\varphi_{qr} \\ I_{dr} = \frac{1}{\sigma L_r}\varphi_{dr} - \frac{M_{sr}}{\sigma L_s L_r}\varphi_{ds} \\ I_{qr} = \frac{1}{\sigma L_r}\varphi_{qr} - \frac{M_{sr}}{\sigma L_s L_r}\varphi_{qs} \\ \omega_s = \frac{d\theta_s}{dt} \end{cases} \quad (11)$$

Where: ω_s and ω_r , denote stator pulsation, rotor pulsation, respectively

The expressions of the electromagnetic torque, active power, and reactive power in the *dq* reference frame are given by the following Equations (12), (13), and (14):

$$C_{em} = \frac{3}{2} P \frac{M}{L_s}\left(\varphi_{qs} I_{dr} - \varphi_{qr} I_{qr}\right) \quad (12)$$

$$\begin{cases} P_s = \frac{3}{2}(V_{ds.} I_{ds} + V_{qs.} I_{qs}) \\ P_r = \frac{3}{2}(V_{dr} I_{dr} + V_{qr} I_{qr}) \end{cases} \quad (13)$$

$$\begin{cases} Q_s = \frac{3}{2}(V_{qs.} I_{ds} + V_{ds.} I_{qs}) \\ Q_r = \frac{3}{2}(V_{qr.} I_{dr} + V_{dr.} I_{qr}) \end{cases} \quad (14)$$

3. VECTOR CONTROL OF DFIG

We demonstrate the ability to control both the active and reactive powers of the machine independently through the direct vector control method. This method involves disregarding the coupling terms and applying a separate controller to each axis. Next, we achieve a vector control system with one controller for each axis, as depicted in Figure 3.

The direct vector control method enables separate control of the active and reactive powers of the electric machine by converting the machine variables into a rotating reference frame. In this dq reference frame, the d-axis current component controls active power, and the q-axis current component controls reactive power. [15], [24] When the coupling terms between the d and q axes are disregarded, the analysis simplifies, focusing solely on the individual effects of each axis., we can create individual PI controllers for each axis. The d-axis PI controller manages the active power by regulating the d-axis current. Similarly, the q-axis PI controller manages the reactive power by regulating the q-axis current.

This decoupled control method significantly simplifies the vector control system's design. Figure 3 illustrates the configuration of a vector control system utilizing one PI controller for each axis. This system allows us to independently regulate both the active and reactive powers of the electric machine.

Implementing decoupled PI control on each axis removes the necessity for intricate feed-forward or model-based control strategies. Furthermore, Figure 4 displays the comprehensive control system for turbine gearboxes.

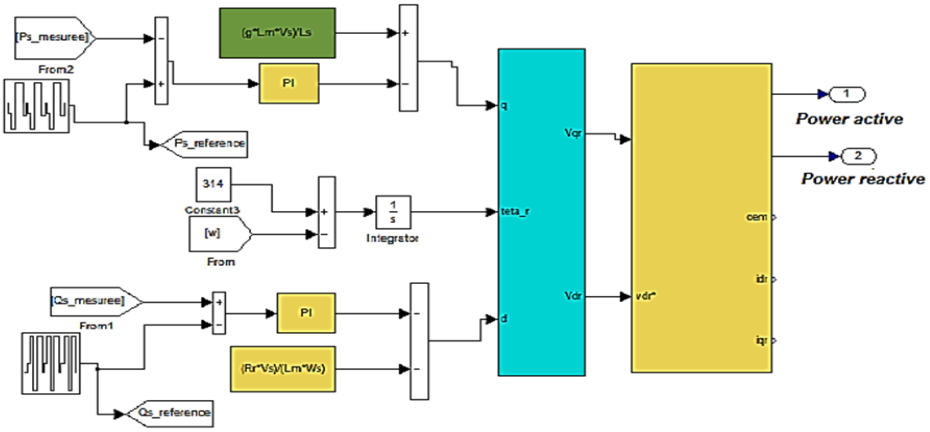

Figure 3. Overall vector control scheme of (DFIG)

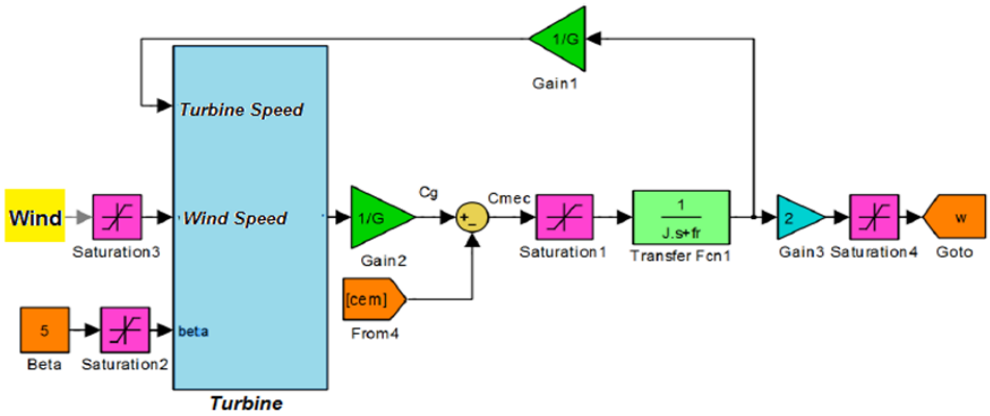

Figure 4. Overall vector control scheme of the turbine

4. SYNTHESIS OF A PROPORTIONAL-INTEGRAL (PI) CONTROLLER

We will now begin creating the controllers needed to implement this control system. A proportional-integral (PI) controller is created. This controller is utilized to regulate the (DFIG) when it is functioning as a generator. Figure 5 displays the system diagram that has been put into practice. The regulator's Kp and Ki gains are determined through pole compensation to achieve a 10 ms response time, which is adequate for our specific application as stated in reference [25]. The open-loop transfer function with regulators is FTBO for the d and q axes.

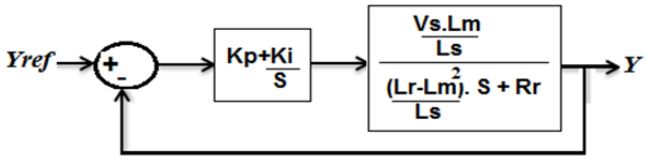

Figure 5. Block diagram of a system with a PI controller

Subsequently, the transfer function for the closed-loop system can be formulated as:

$$FTCL = \frac{1}{1+\tau_r.S} \quad (15)$$

With: $\tau_r = \frac{L_s(L_r - \frac{L_m^2}{L_s})}{K_p L_m V_s}$

The controllers' gains are determined by the machine parameters and the desired response time.

$$\begin{cases} K_p = \frac{L_s(L_r - \frac{L_m^2}{L_s})}{\tau_r L_m V_s} \\ K_i = \frac{L_s R_r}{\tau_r L_m V_s} \\ \frac{K_i}{K_p} = \frac{L_s R_r}{L_s(L_r - \frac{L_m^2}{L_s})} \end{cases} \quad (16)$$

5. CONTROLING THE DFIG MACHINE USING NEURAL PI

ANNs mimic the human brain's structure, using interconnected artificial neurons. These networks feature weight-based connections, analogous to synapses. While a single hidden layer can model any function, optimal network architecture is determined empirically. ANNs can have diverse structures with multiple layers, adapting to various computational tasks.[26], [27], [28].The mathematical model for a neuron in the ll-th layer is given by:

$$Y_j^i = f\left(\sum_i^{nl} W_{ji}^l X_i + b_j^i\right) \quad (17)$$

This work uses a Multi-Layer Perceptron network composed of several layers. The input layer receives data, followed by hidden layers between the input and output, all in a feed-forward structure without feedback connections. The final layer provides the desired outputs.[29], [30], [31].

The proposed static MLP neural controller, shown in Figure.6, features the input layer consisting of 2 neurons,one for wind speed and the other for mechanical speed, two hidden layers with hyperbolic sigmoid functions (as in equation 18), and a single neuron in the output layer for reference electromagnetic torque using a linear function. Optimal results are achieved with a configuration of one neuron in the input and output layers and a hidden layer with three neurons (Figure.7), due to the structural similarity between Layers 1 and 3.[29], [30], [32].

$$sgm = \frac{1-\exp(-2x)}{1+\exp(-2x)} \quad (18)$$

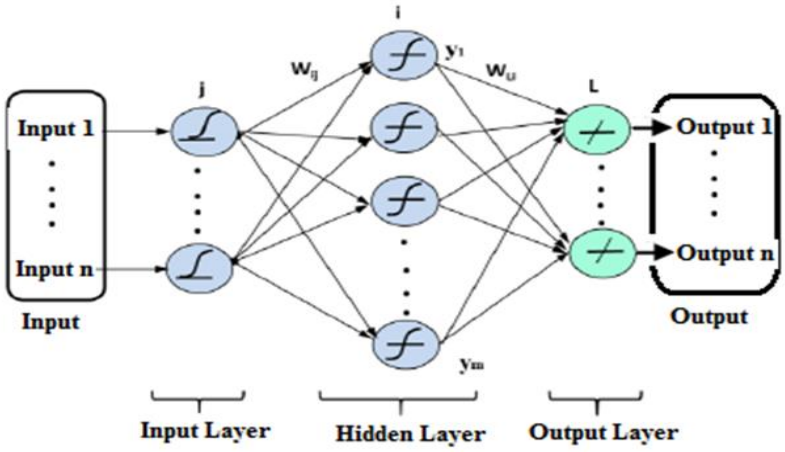

Figure 6. Structure of a Standard Neural Network

The data was divided into 70% training, 15% testing, and 15% validation. The MLP, shown in Figure.(8a), was trained with the Levenberg-Marquardt algorithm for its efficiency and reliability. [8], [29]. Training was limited to 100 iterations, as further iterations did not enhance performance.

As shown in Figure (8b), the proposed structure (2-5-5-5-1) quickly converged to the optimal solution by the 30th iteration, with minimal error variation afterward, reaching an error of 3.62×10−4. The total number of iterations was set to 100.

Neural network control involves designing a neural network controller based on an existing proportional-integral (PI) controller. The neural network is trained to replicate the input-output behavior of the PI controller. The Levenberg-Marquardt algorithm is used to optimize the network by adjusting its parameters (weights and biases) to minimize the error between the neural network and PI controller outputs.

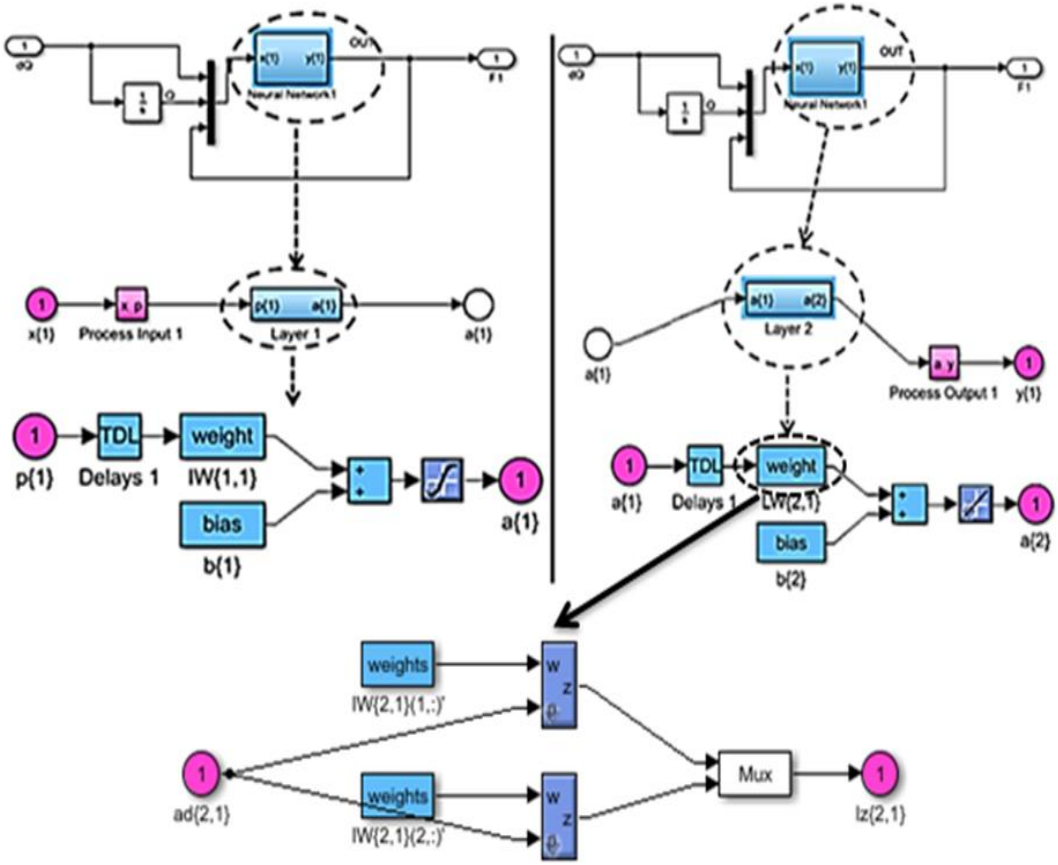

Figure 7. Block diagram of numerical controller ANN

The training process iteratively updates the network parameters to minimize the mean squared error between the PI controller's target output and the neural network output. The Levenberg-Marquardt algorithm efficiently navigates the error surface to find the optimal parameter set that reduces network error. Once trained, the neural network can mimic the PI controller's response to various system disturbances and operating conditions using the learned weights and biases. Neural networks surpass traditional PI controllers by capturing complex, nonlinear system behaviors more effectively.

The neural controller demonstrates greater adaptability and resilience across a broad spectrum of operating conditions compared to the PI controller. Neural network control utilizing pre-existing proportional-integral knowledge offers a more robust and adaptable control solution. [8], [27], [28].

Figure 9 illustrates the general layout of direct vector control with neural network controllers.

Training a neural network involves modifying its behavior to approach a specific objective. Typically, this objective is accomplished by either approximating a group of examples or optimizing the network's state by adjusting its weights to reach the minimum of a predefined cost function. Training procedures are utilized to establish the network parameters to ensure appropriate behavior for specific inputs based on the level of supervision applied during training. [33], [34], [35].

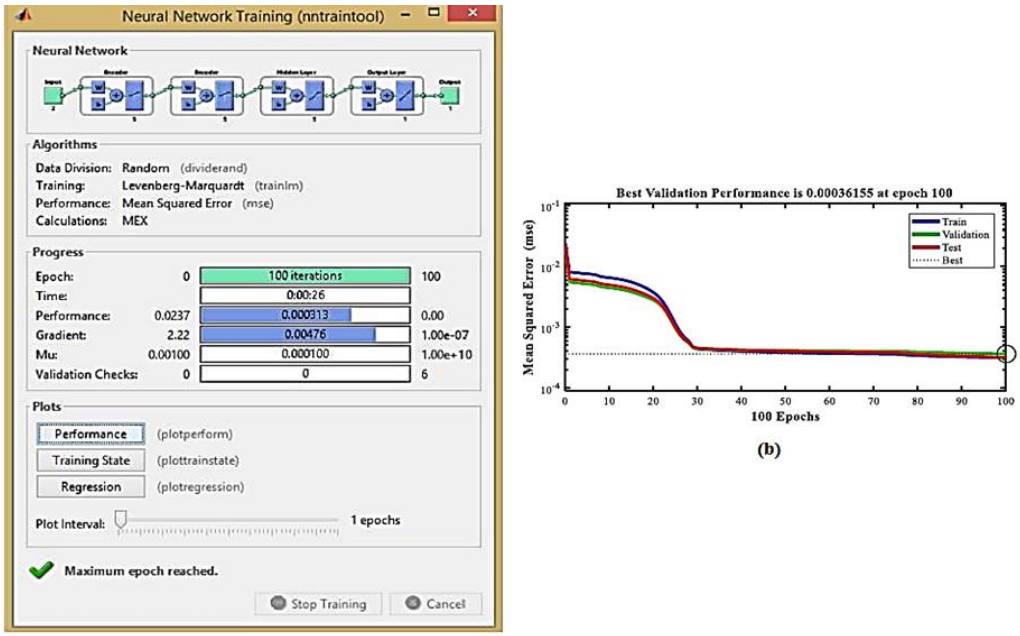

Figure 8. (a): ANN learning progress, (b): Performance curve of training

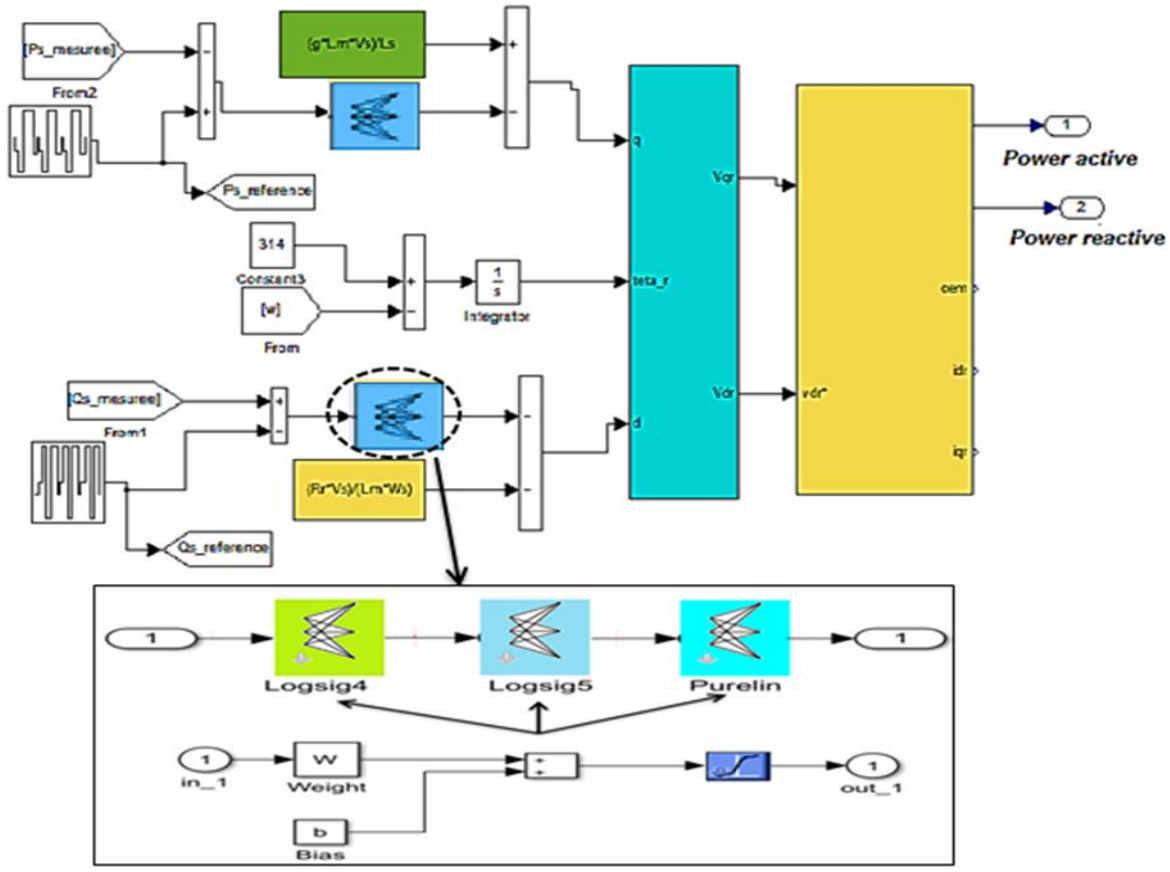

Figure 9. Direct vector control of a DFIG with neural network controllers

6. RESULTS. AND DISCUSSION

The wind system was modeled using MATLAB/Simulink software. Implementing or simulating wind energy conversion is essential for validating our theoretical research. The stator of the machine is linked

directly to the three-phase grid. A Pulse-Width Modulation (PWM)-controlled three-phase inverter drives the rotor. Table 1 contains the parameters for the DFIG and turbine system.

The parameters are selected to ensure optimal performance of the wind power system (Turbine/DFIG). Mechanical values like viscous friction coefficient, moment of inertia, and turbine radius are crucial for determining the system's response and efficiency in converting wind energy to mechanical energy. Meanwhile, electrical characteristics such as winding resistances and self-inductances directly impact power generation efficiency and system performance, ensuring the system operates effectively at its nominal power rating.

Table 1. Parameters of a wind power system [22]

TURBINE	
Coefficient of viscous friction of the DFIG.	f= 0,0024 N*m.s^{-1}
Inertia of the shaft.	J= 1000 Kg .m^2
Wind turbine radius.	R= 35.25 m.
Gain of the speed multiplier.	G= 90
Air density	ρ = 1.225 Kg/m^3
DFIG	
Stator. resistance per phase	Rs= 0,012 Ω
Rotor. resistance per phase	Rr= 0,021 Ω
Self-.inductance of the stator per phase	Ls= 0,0137 mH
Self-.inductance of the rotor per phase	Lr= 0,0136 mH
Mutual inductance	M= 0,0135
Nominal power	1,5 MW

We connected our Doubly Fed Induction Generator (DFIG) to a turbine operating at a constant mechanical speed, approximately equal to 180 rad/s, Figure 9.

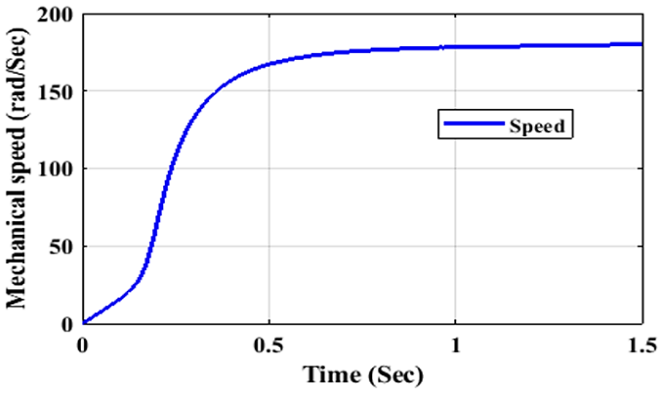

Figure 9. Mechanical turbine's speed

Figures (10) and (11) display the system's responses using two controllers. The generator, equipped with both controllers, effectively carries out the active and reactive power adjustments.Upon closer examination; it is evident that the neural controller has a quicker rise time compared to both control types, which exhibit similar overshoot. The PI controller is slightly more effective for active power; whereas the neural controller exhibits reduced overshoot in reactive power.

The neural scheme is favored due to differences in response time and steady-state error. Both the power tracking and disturbance rejection are sufficient. The PI control exhibits increased oscillations, but maintains continuous tracking of the reference signal in steady-state compared to the neural control. The simulations confirm that the adaptive-parameter neural controller is superior because of its fast response speed. The PI controller improves steady-state performance by providing smoother responses and reducing errors.

The stator reactive power (Qreal, QNeural) is dependent on the direct rotor current Idr. The stator, active power (Preal, PNeural) is dependent on the quadrature rotor current (Idr, IdrN) and (Iqr, IqrN) figure (12). When the active or reactive power changes quickly because of the inverter rotor switches switching on and off, the d and q control axes move back and forth in small waves.

The stator active power depends on both the actual and neural network-based quadrature rotor currents, as depicted in the figure 12. The stator's reactive power depends on the direct rotor current. Both scenarios exhibit a noticeable impact of coupling between the d-axis and q-axis controls. Minor oscillations

occur when there is a sudden change in active or reactive power due to the switching of rotor inverter switches.

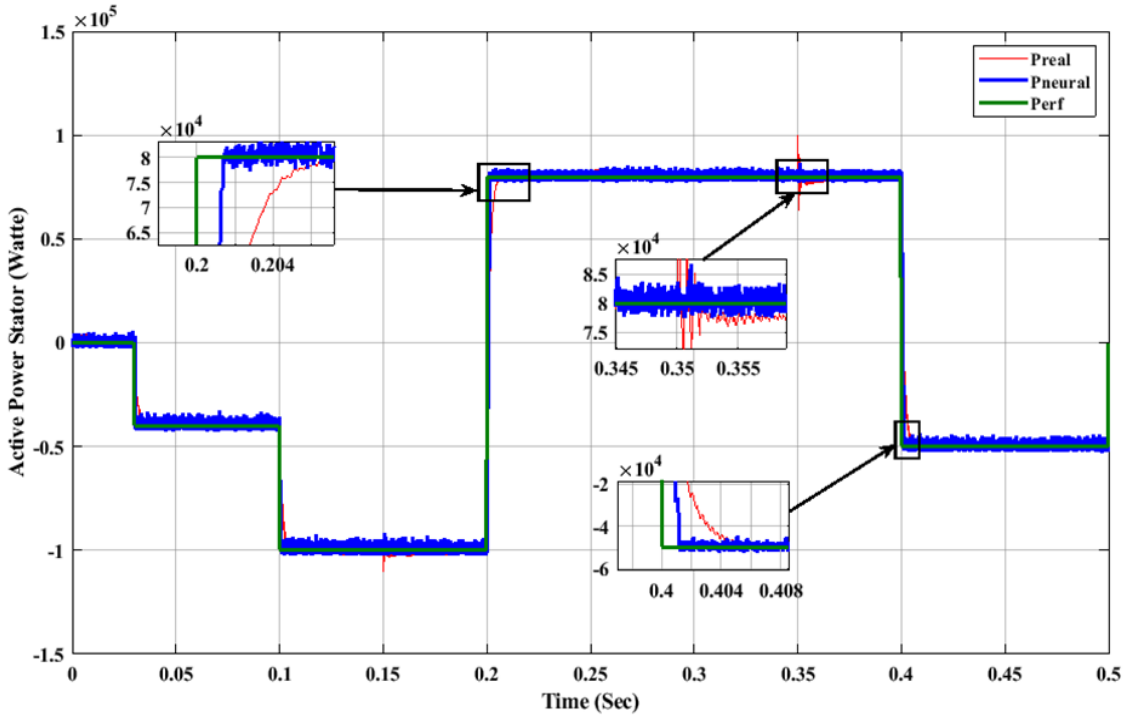

Figure 10. Active Power Performance (Direct Vector and Neural Network)

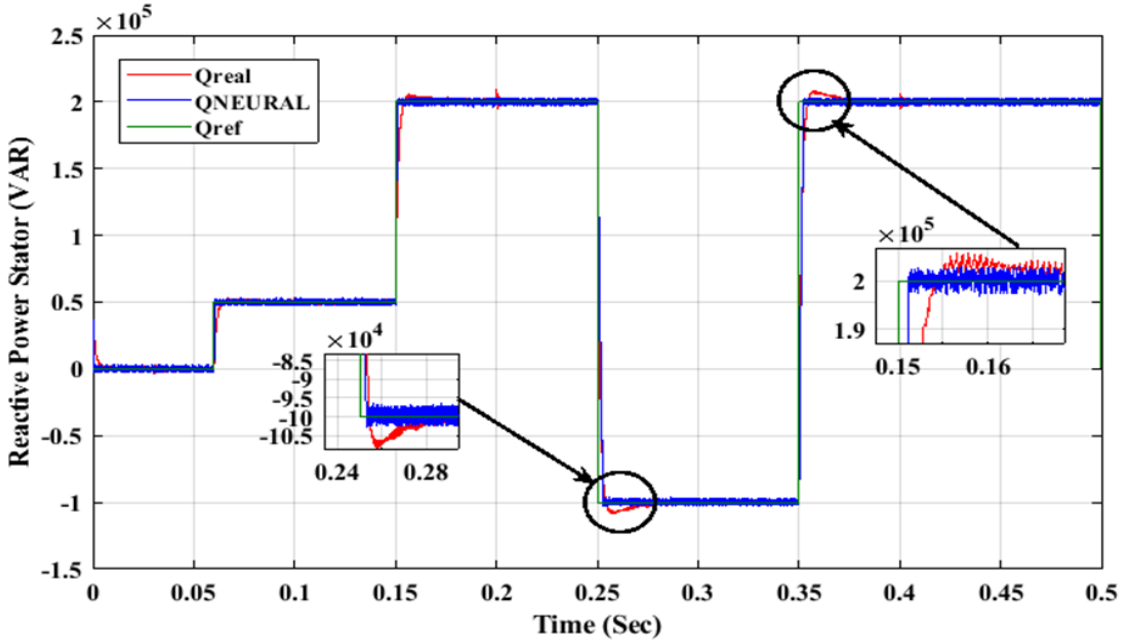

Figure 11. Reactive Power Performance (Direct Vector and Neural Network)

Figure 13 displays the electromagnetic torque outcomes for the DFIG controlled by direct vector and neural network methods. The neural network control exhibits quicker rise time and settling time in response to torque. Vector control offers increased damping but exhibits slower dynamics. Both methods accurately monitor the torque reference under stable conditions, while the adaptive neural network controller shows enhanced transient performance.

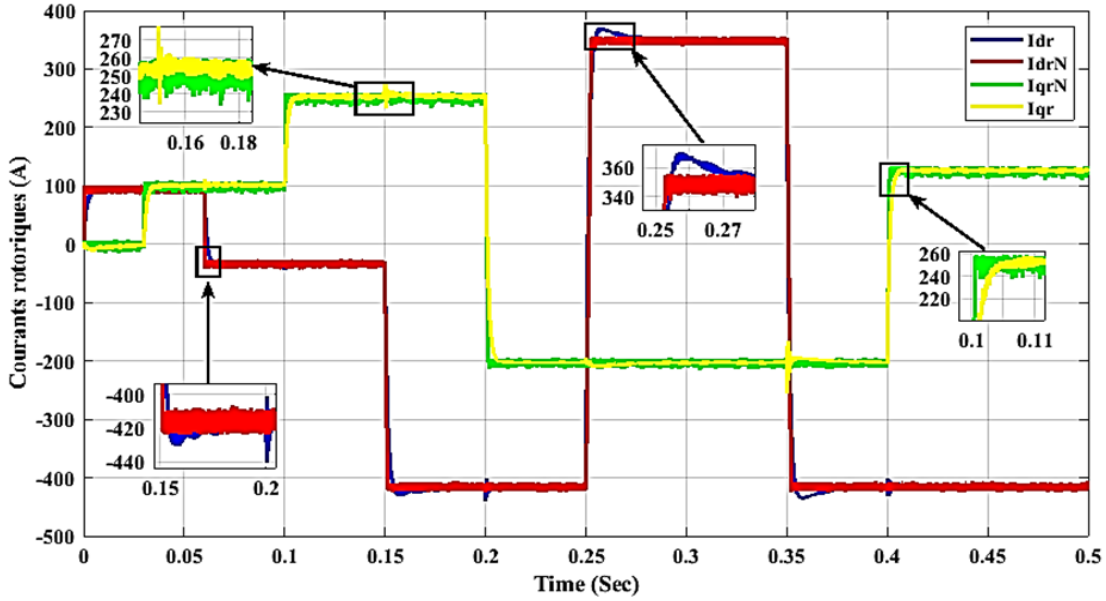

Figure 12. Rotor Currents (Vector Control and Neural Network Control)

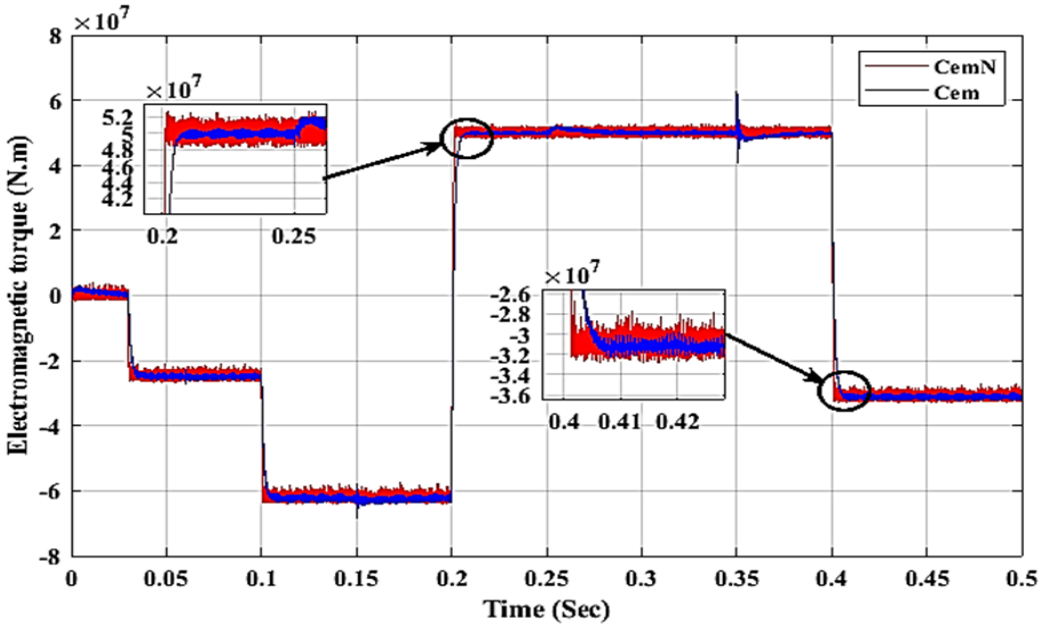

Figure 13. DFIG Electromagnetic Torque (Vector Control and Neuron)

7. A COMPARATIVE STUDY OF THE PROPOSED NEURAL NETWORK TECHNIQUE AND EXISTING RESEARCH PAPERS

Table 2 compares the proposed methodology for regulating active and reactive power in doubly-fed induction generators using artificial neural network controllers with other techniques such as RBFFNN, ISMC, NDVC, and RT2FNN. The comparison is based on the system's response time.

Based on the results presented in the table, it is observed that the proposed technique using Artificial Neural Network (ANN) controllers is the most effective compared to the other methods. The proposed technique shows the fastest response time for both active and reactive power, with a response time of 0.025s for active power and 0.018 seconds for reactive power. In contrast, other techniques such as RBFFNN, ISMC, NDVC, and RT2FNN are less efficient, with active power response times ranging from 0.051 seconds to 1.78 seconds, highlighting the superiority of ANN in dynamic control.

The table.3 presents a comparison of various techniques for reducing ripples in P and Q . The ANN (Artificial Neural Network) technique used in the current study, titled "Regulation of active and reactive

powers in doubly-fed induction generators utilizing proportional-integral and artificial neural network controllers", demonstrates noteworthy performance.

This technique achieved high reduction rates of 75% for active power and 80% for reactive power. These figures indicate noteworthy efficacy of the ANN technique in improving the performance of doubly-fed induction generators. The results showcase ANN's capability to achieve a good balance in ripple reduction for both active and reactive power, thereby enhancing power regulation efficiency in these systems.

This performance underscores the promising potential of ANN in the field of power quality improvement and regulation in electrical power generation systems. The high reduction rates achieved by ANN highlight its effectiveness in addressing power quality issues and optimizing the operation of doubly-fed induction generators.

Table 2. Comparison of response times for Active and Reactive power

Technique	P response time [s]	Q response time [s]	Reference paper
ANN	0.025	0.018	Proposed technique
ANN	0.028	0.021	**[28]**
RBFFNN	1.33	/	**[36]**
ISMC	0.051	0.052	**[8]**
NDVC	1, 78	/	**[37]**
RT2FNN	1.7	/	**[38]**

Table 3. Comparison of ripple reduction rates

Technique	Ratios (%)		Reference
	Active power (W)	Reactive power (VAR)	
ANN	75	80	Current study
DRAPC-MSCT	73.33	84.50	**[39]**
Backstepping control	28.57	46.93	**[40]**
DPC-ANN	66.29	66.29	**[41]**
DPC-NF	57.74	67.13	**[41]**

8. CONCLUSION

This paper looks at the similarities and differences between PI controllers and neural network controllers in order to control doubly-fed induction generator wind turbines. When induction generators power wind turbines, PI controllers are used to steer them. It is possible to separate power sources by using indirect rotor vector control, but PI control is not very reliable. It is possible to separate power sources. We show how to build a neural network that uses backpropagation to make it work better, respond faster, and be able to handle changes in parameters over PI control with only slightly bigger oscillations. This building's design is shown here. You can read about this architecture in this paper. One way to show this point is through the use of simulations.

REFERENCES

[1] M. Bouderbala, B. Bossoufi, A. Lagrioui, M. Taoussi, H. A. Aroussi, and Y. Ihedrane, 'Direct and indirect vector control of a doubly fed induction generator based in a wind energy conversion system', *International Journal of Electrical and Computer Engineering (IJECE)*, vol. 9, no. 3, Art. no. 3, Jun. 2019, doi: 10.11591/ijece.v9i3.pp1531-1540.

[2] C. Oudaa, E. I. A. Mahmoud, A. K. K. Mahmoud, C. B. D. Eddine, and B. Azeddine, 'Optimal Control Technique of an Induction Motor', *Indonesian Journal of Electrical Engineering and Informatics (IJEEI)*, vol. 11, no. 2, Art. no. 2, Jun. 2023, doi: 10.52549/ijeei.v11i2.4447.

[3] H. Sediki, D. O. Abdeslam, T. Otmane-cherif, A. Bechouche, and K. Mesbah, 'Steady-State Analysis and Control of Double Feed Induction Motor', Jan. 2012, doi: 10.5281/zenodo.1063036.

[4] A. Zemmit, R. Sadouni, and A. Meroufel, 'Direct Torque Control of Double Feed Induction Machine (DTC-DFIM)', *JARST*, vol. 2, no. 2, pp. 204–209, Jun. 2015, Accessed: Feb. 26, 2024. [Online]. Available: https://www.asjp.cerist.dz/en/article/4955

[5] S. Li, H. Wang, Y. Tian, A. Aitouch, and J. Klein, 'Direct power control of DFIG wind turbine systems based on an intelligent proportional-integral sliding mode control', *ISA Transactions*, vol. 64, pp. 431–439, Sep. 2016, doi: 10.1016/j.isatra.2016.06.003.

[6] M. Ćalasan, S. H. E. Abdel Aleem, and A. F. Zobaa, 'A new approach for parameters estimation of double and triple diode models of photovoltaic cells based on iterative Lambert W function', *Solar Energy*, vol. 218, pp. 392–412, Apr. 2021, doi: 10.1016/j.solener.2021.02.038.

[7] M. Bouzidi, A. Harrouz, and S. Mansouri, 'Control and automation of Asynchronous motor using Fuzzy logic', *1*, vol. 1, no. 02, Art. no. 02, Dec. 2019, Accessed: Feb. 26, 2024. [Online]. Available: https://ajresd.univ-adrar.edu.dz/index.php?journal=AJRESD&page=article&op=view&path[]=44

[8] H. Chojaa, A. Derouich, S. E. Chehaidia, O. Zamzoum, M. Taoussi, and H. Elouatouat, 'Integral sliding mode control for DFIG based WECS with MPPT based on artificial neural network under a real wind profile', *Energy Reports*, vol. 7, pp. 4809–4824, Nov. 2021, doi: 10.1016/j.egyr.2021.07.066.
[9] H. Benbouhenni, Z. Boudjema, and A. Belaidi, 'Direct vector control of a DFIG supplied by an intelligent SVM inverter for wind turbine system', *Iranian Journal of Electrical and Electronic Engineering*, vol. 15, pp. 45–55, Mar. 2019, doi: 10.22068/IJEEE.15.1.45.
[10] A. Herizi, R. Rouabhi, and A. Zemmit, 'Speed control of doubly fed induction motor using backstepping control with interval type-2 fuzzy controller', *Diagnostyka*, vol. 24, no. 3, pp. 1–8, Jun. 2023, doi: 10.29354/diag/166460.
[11] A. Junyent-Ferré, O. Gomis-Bellmunt, A. Sumper, M. Sala, and M. Mata, 'Modeling and control of the doubly fed induction generator wind turbine', *Simulation Modelling Practice and Theory*, vol. 18, no. 9, pp. 1365–1381, Oct. 2010, doi: 10.1016/j.simpat.2010.05.018.
[12] F. Moulay, A. Habbatti, and H. Hamdaoui, 'Application and Control of a Doubly Fed Induction Machine Integrated in Wind Energy System', *I2M*, vol. 18, no. 3, pp. 257–265, Aug. 2019, doi: 10.18280/i2m.180305.
[13] M. Lamnadi, M. Trihi, B. Bossoufi, and A. Boulezhar, 'Modeling and Control of a Doubly-Fed Induction Generator for Wind Turbine-Generator Systems', *International Journal of Power Electronics and Drive Systems (IJPEDS)*, vol. 7, no. 3, Art. no. 3, Sep. 2016, doi: 10.11591/ijpeds.v7.i3.pp982-995.
[14] N. O. Farrar, M. H. Ali, and D. Dasgupta, 'Artificial Intelligence and Machine Learning in Grid Connected Wind Turbine Control Systems: A Comprehensive Review', *Energies*, vol. 16, no. 3, Art. no. 3, Jan. 2023, doi: 10.3390/en16031530.
[15] E. Chetouani, Y. Errami, A. Obbadi, and S. Sahnoun, 'Self-adapting PI controller for grid-connected DFIG wind turbines based on recurrent neural network optimization control under unbalanced grid faults', *Electric Power Systems Research*, vol. 214, p. 108829, Jan. 2023, doi: 10.1016/j.epsr.2022.108829.
[16] M. S. Nazir, Y. Wang, A. J. Mahdi, X. Sun, C. Zhang, and A. N. Abdalla, 'Improving the Performance of Doubly Fed Induction Generator Using Fault Tolerant Control—A Hierarchical Approach', *Applied Sciences*, vol. 10, no. 3, Art. no. 3, Jan. 2020, doi: 10.3390/app10030924.
[17] H. Benbouhenni, Z. Boudjema, and A. Belaidi, 'Indirect Vector Control of a DFIG Supplied by a Two-level FSVM Inverter for Wind Turbine System', *Majlesi Journal of Electrical Engineering*, vol. 13, no. 1, pp. 45–54, Mar. 2019, Accessed: Jun. 21, 2024. [Online]. Available: https://mjee.isfahan.iau.ir/article_696337.html
[18] O. Djaidja, H. Mekki, S. Zeghlache, and A. Djerioui, 'A new improved control for power quality enhancement in double fed induction generator using iterative learning control', *Diagnostyka*, vol. 24, no. 3, pp. 1–8, Aug. 2023, doi: 10.29354/diag/169462.
[19] Y. K. Wu and W.-H. Yang, 'Different Control Strategies on the Rotor Side Converter in DFIG-based Wind Turbines', *Energy Procedia*, vol. 100, pp. 551–555, Nov. 2016, doi: 10.1016/j.egypro.2016.10.217.
[20] A. Akhbari, M. Rahimi, and M. H. Khooban, 'Direct current grid-based doubly-fed induction generator wind turbines: Real-time control and stability analysis', *IET Power Electronics*, vol. 15, no. 12, pp. 1158–1173, 2022, doi: 10.1049/pel2.12299.
[21] F. Arama, A. Fatima Zohra, S. Laribi, Z. Seddik, and H. Messaoud, 'Control of Doubly Fed Induction Generator for Wind Turbine', Mar. 2020.
[22] A. Chandad, M. Hamouda, N. Benharir, and M. Bouzidi, 'Enhancing of a wind power system control using intelligent artificial control and multilayer inverter', *International Journal of Power Electronics and Drive Systems (IJPEDS)*, vol. 15, no. 3, Art. no. 3, Sep. 2024, doi: 10.11591/ijpeds.v15.i3.pp1959-1967.
[23] H. Benbouhenni, Z. Boudjema, and A. Belaidi, 'Indirect Vector Control of a DFIG Supplied by a Two-level FSVM Inverter for Wind Turbine System', *Majlesi Journal of Electrical Engineering*, vol. 13, no. 1, pp. 45–54, Mar. 2019, Accessed: Feb. 26, 2024. [Online]. Available: https://mjee.isfahan.iau.ir/article_696337.html
[24] G. S. Kaloi, J. Wang, and M. H. Baloch, 'Active and reactive power control of the doubly fed induction generator based on wind energy conversion system', *Energy Reports*, vol. 2, pp. 194–200, Nov. 2016, doi: 10.1016/j.egyr.2016.08.001.
[25] H. Mesai-ahmed, A. Bentaallah, A. J. M. Cardoso, Y. Djeriri, and I. Jlassi, 'Robust Neural Control of the Dual Star Induction Generator Used in a Grid-Connected Wind Energy Conversion System', *MMEP*, vol. 8, no. 3, pp. 323–332, Jun. 2021, doi: 10.18280/mmep.080301.
[26] M. Bouzidi, H. Abdelkader, S. Mansouri, and V. Dumbrava, 'Modeling of a Photovoltaic Array with Maximum Power Point Tracking Using Neural Networks', *Applied Mechanics and Materials*, vol. 905, pp. 53–64, 2022, doi: 10.4028/p-ndl3bi.
[27] K. M. Elbachir and A. Ahmed, 'Artificial Neural Networks Direct Torque Control of Single Inverter Feed Two Induction Motors', *JESA*, vol. 54, no. 6, pp. 881–889, Dec. 2021, doi: 10.18280/jesa.540610.
[28] 'Active and Reactive Powers Control of DFIG Based WECS Using PI Controller and Artificial Neural Network Based Controller | IIETA'. Accessed: Sep. 02, 2024. [Online]. Available: https://www.iieta.org/journals/mmc_a/paper/10.18280/mmc_a.931-405
[29] S. E. Chehaidia, A. Abderezzak, H. Kherfane, B. Boukhezzar, and H. Cherif, 'AN IMPROVED MACHINE LEARNING TECHNIQUES FUSION ALGORITHM FOR CONTROLS ADVANCED RESEARCH TURBINE (CART) POWER COEFFICIENT ESTIMATION'.
[30] B. Meghni, H. Chojaa, and A. Boulmaiz, 'An Optimal Torque Control based on Intelligent Tracking Range (MPPT-OTC-ANN) for Permanent Magnet Direct Drive WECS', in *2020 IEEE 2nd International Conference on Electronics, Control, Optimization and Computer Science (ICECOCS)*, Dec. 2020, pp. 1–6. doi: 10.1109/ICECOCS50124.2020.9314304.

[31] L. Xiong, J. Wang, X. Mi, and M. W. Khan, 'Fractional Order Sliding Mode Based Direct Power Control of Grid-Connected DFIG', *IEEE Transactions on Power Systems*, vol. 33, no. 3, pp. 3087–3096, May 2018, doi: 10.1109/TPWRS.2017.2761815.
[32] A. Dahbi, N. Nait-Said, and M.-S. Nait-Said, 'A novel combined MPPT-pitch angle control for wide range variable speed wind turbine based on neural network', *International Journal of Hydrogen Energy*, vol. 41, no. 22, pp. 9427–9442, Jun. 2016, doi: 10.1016/j.ijhydene.2016.03.105.
[33] K. K. Ilse, B. W. Figgis, V. Naumann, C. Hagendorf, and J. Bagdahn, 'Fundamentals of soiling processes on photovoltaic modules', *Renewable and Sustainable Energy Reviews*, vol. 98, pp. 239–254, Dec. 2018, doi: 10.1016/j.rser.2018.09.015.
[34] O. A. Montesinos López, A. Montesinos López, and J. Crossa, 'Fundamentals of Artificial Neural Networks and Deep Learning', in *Multivariate Statistical Machine Learning Methods for Genomic Prediction*, O. A. Montesinos López, A. Montesinos López, and J. Crossa, Eds., Cham: Springer International Publishing, 2022, pp. 379–425. doi: 10.1007/978-3-030-89010-0_10.
[35] S. Aoun, A. Boukadoum, and L. Yousfi, 'Advanced power control of a variable speed wind turbine based on a doubly fed induction generator using field-oriented control with fuzzy and neural controllers', *International Journal of Dynamics and Control*, pp. 1–14, Nov. 2023, doi: 10.1007/s40435-023-01345-9.
[36] D. Khan, J. Ahmed Ansari, S. Aziz Khan, and U. Abrar, 'Power Optimization Control Scheme for Doubly Fed Induction Generator Used in Wind Turbine Generators', *Inventions*, vol. 5, no. 3, Art. no. 3, Sep. 2020, doi: 10.3390/inventions5030040.
[37] H. Benbouhenni and N. Bizon, 'Advanced Direct Vector Control Method for Optimizing the Operation of a Double-Powered Induction Generator-Based Dual-Rotor Wind Turbine System', *Mathematics*, vol. 9, no. 19, Art. no. 19, Jan. 2021, doi: 10.3390/math9192403.
[38] J. Tavoosi *et al.*, 'A machine learning approach for active/reactive power control of grid-connected doubly-fed induction generators', *Ain Shams Engineering Journal*, vol. 13, no. 2, p. 101564, Mar. 2022, doi: 10.1016/j.asej.2021.08.007.
[39] H. Benbouhenni, N. Bizon, I. Colak, M. I. Mosaad, and M. Yessef, 'Direct active and reactive powers control of double-powered asynchronous generators in multi-rotor wind power systems using modified synergetic control', *Energy Reports*, vol. 10, pp. 4286–4301, Nov. 2023, doi: 10.1016/j.egyr.2023.10.085.
[40] H. Benbouhenni, H. Gasmi, and I. Colak, 'Intelligent Control Scheme of Asynchronous Generator-Based Dual-Rotor Wind Power System Under Different Working Conditions', *Majlesi Journal of Energy Management*, vol. 11, no. 3, Art. no. 3, 2022, Accessed: Sep. 03, 2024. [Online]. Available: https://em.majlesi.info/index.php/em/article/view/494
[41] F. Echiheb *et al.*, 'Robust sliding-Backstepping mode control of a wind system based on the DFIG generator', *Sci Rep*, vol. 12, no. 1, p. 11782, Jul. 2022, doi: 10.1038/s41598-022-15960-7.

BIOGRAPHY OF AUTHORS

Dr. Mohammed Bouzidi, was born in 1981 in Algeria. He obtained his Master's degree in Electrical Engineering with a specialization in Automation Control from the University of Béchar in 2015. Later, in 2023, he earned his Ph.D. in Electrical Engineering from the University of Adrar. He began his professional career as a secondary school technical education teacher from 2005 to 2017. Currently, he works as an Associate Professor at Tamanrasset University in Algeria at the Faculty of Science and Technology. In addition to his teaching role, he has published numerous research papers in the field of electrical engineering. His primary research interests include diagnosing renewable energy systems and controlling electrical machines.
You can contact him at email: : mohbouzidi81@yahoo.fr

Pr. Abdulfatah Nassri, was born in 1978 in Bechar, Algeria. He is a full professor in the Department of Electrical Engineering at the Faculty of Science and Technology, University of Bechar - Algeria. He is considered an active member in the laboratory Smart Grid and Renewable Energy SGRE University Tahri Mohamed Bechar Algeria and is an author and co-author of numerous published research papers in the fields of smart grids and renewable energy. He can be contacted via email at: nasri.abdelfatah@univ-bechar.dz.

Dr. Oussama Hafsi, born in 1991, obtained his PhD in 2022 from the University of Bechar, specializing in Smart Grids and Renewable Energies. His research interests include: DC-Microgrid, Renewable Energies, power electronic converters, control and management of energy systems. He is currently working as a lecturer at the Faculty of Science and Technology, University of Adrar, Algeria.
He can be contacted via email at: oussama5bm@gmail.com

Dr. Boubaker Faradj obtained his PhD in Electrical Engineering from the University of Laghouat, Algeria in 2019. He is currently working as a lecturer at the University of Tamanghasset; main field of research is reluctance machines in renewable energy. He has conducted extensive research in the areas of electrical machine modeling, electrical drive control, fault diagnosis, smart grids, and renewable energy systems.
He can be contacted via email at: boubakarluck@yahoo.fr